Estimation of the Device Gamut of a Digital Camera in Raw Performance Using Optimal Color-Stimuli

Jaume Pujol[a], Francisco Martínez-Verdú[b] and Pascual Capilla[c]
[a] Center for Development of Sensors, Instrumentation and Systems,
Dept. of Optics and Optometry, Technical University of Catalonia
Terrassa, Barcelona, Spain
[b] Dept. of Optics, University of Alicante, Alicante, Spain
[c] Dept. of Optics, University of Valencia, Burjassot, Valencia, Spain

Abstract

Using a spectroradiometric model of capture for a digital camera based on the mathematical description of the empirical opto-electronic conversion spectral functions (OECSF), the capture of MacAdam or optimal spectra with fixed illumination level is simulated. This model of capture allows to change freely the f-number of the zoom-lens and/or the photosite integration time of the electronic shutter of the camera, regardless of the spectral composition of the stimulus. If we follow the procedure employed by MacAdam in 1935 working with the CIE-1931 XYZ standard observer, these color-stimuli are arranged in decreasing pyramidal form as the luminance factor increases for any chromaticity diagram (CIE-xy, UCS-u'v' or CIE-L*a*b*). These loci are often called MacAdam limits or Rösch color solid. On the other hand, transforming the simulated RGB digital output levels of the optimal colors to XYZ data through the raw colorimetric profile with luminance adaptation of our digital image capture device, the corresponding MacAdam loci for each luminance factor are smaller than those of the colorimetric standard observer. This systematic desaturation of the optimal color-stimuli shows that our color device, in raw performance, desaturates in general the real color-stimuli, so this result justifies the additional use in digital photography of color correction algorithms, more or less complex, in order to reach the colorimetric status of color reproduction.

Introduction

Optimal or MacAdam color-stimuli[1,2] are binary (zero or one) spectral profiles of reflectance or transmittance. There are two kinds of these color-stimuli: type 1, when $\rho(\lambda) = 1$ for $\lambda \in [\lambda_1 , \lambda_2]$ nm, and, type 2, when $\rho(\lambda) = 1$ for $\lambda \notin]\lambda_1 , \lambda_2]$ nm (Fig. 1).
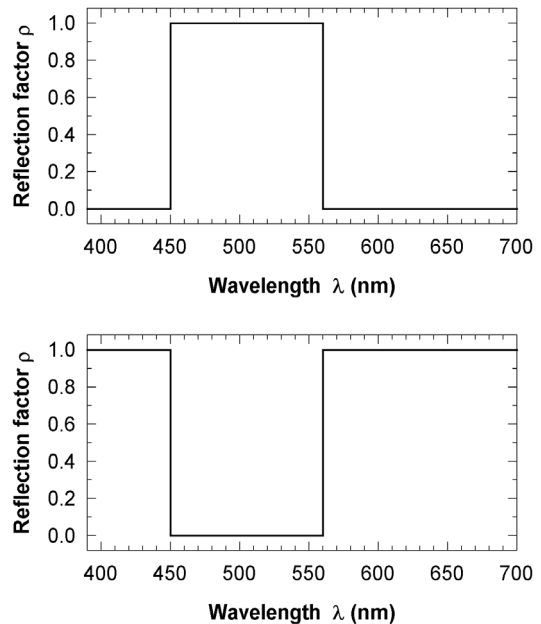

Figure 1. Two samples of optimal color-stimuli with luminance factor Y = 50: type 1 (top) and type 2 (bottom).

Using a vector space notation[3] the algorithm obtaining the optimal color-stimuli is as follows. Selecting the spectral range equals to [380, 780] nm at 1 nm step, the length of the color-stimuli vectors will be 401. Considering the color-matching functions $\mathbf{T}_{XYZ}$ of the CIE-1931 XYZ standard observer and the equal-energy illuminant $\mathbf{E}$, the two types of optimal color-stimuli are redistributed according to its luminance factor Y as follows:

$\lambda \in [380, 780]\,\text{nm}$

$\Delta\lambda = 1\,\text{nm}$

$N = \dfrac{780 - 380}{\Delta\lambda} + 1 = 401$

$\mathbf{T_{XYZ}} = \begin{bmatrix} \bar{\mathbf{x}} & \bar{\mathbf{y}} & \bar{\mathbf{z}} \end{bmatrix}_{401 \times 3}$

$\mathbf{E} = \begin{bmatrix} 1 & 1 & \cdots & 1 \end{bmatrix}^{t}$

; TYPE 1

$for\ Y = 1\ to\ \{10, 20, \ldots, 80, 90, 95\}\ do$

    $for\ i = 1\ to\ N\ do$

        $for\ j = 1\ to\ N\ do$

$if\ i < j\ and\ \dfrac{100}{\left(\bar{\mathbf{y}}^{t} \cdot \mathbf{E}\right)} \sum_{k=i}^{j} \bar{\mathbf{y}}(\lambda_k) \in [Y - 0.05, Y + 0.05]$

$then\ save\ (i \equiv \lambda_1,\ j \equiv \lambda_2)$

        $end\ for$

    $end\ for$

$end\ for$

; TYPE 2

$for\ Y = 1\ to\ \{10, 20, \ldots, 80, 90, 95\}\ do$

    $for\ i = 1\ to\ N\ do$

        $for\ j = 1\ to\ N\ do$

$if\ i < j\ and\ \dfrac{100}{\left(\bar{\mathbf{y}}^{t} \cdot \mathbf{E}\right)} \left[\sum_{k=1}^{i} \bar{\mathbf{y}}(\lambda_k) + \sum_{k=j}^{N} \bar{\mathbf{y}}(\lambda_k) \right] \in [Y - 0.05, Y + 0.05]$

$then\ save\ (i \equiv \lambda_1,\ j \equiv \lambda_2)$

        $end\ for$
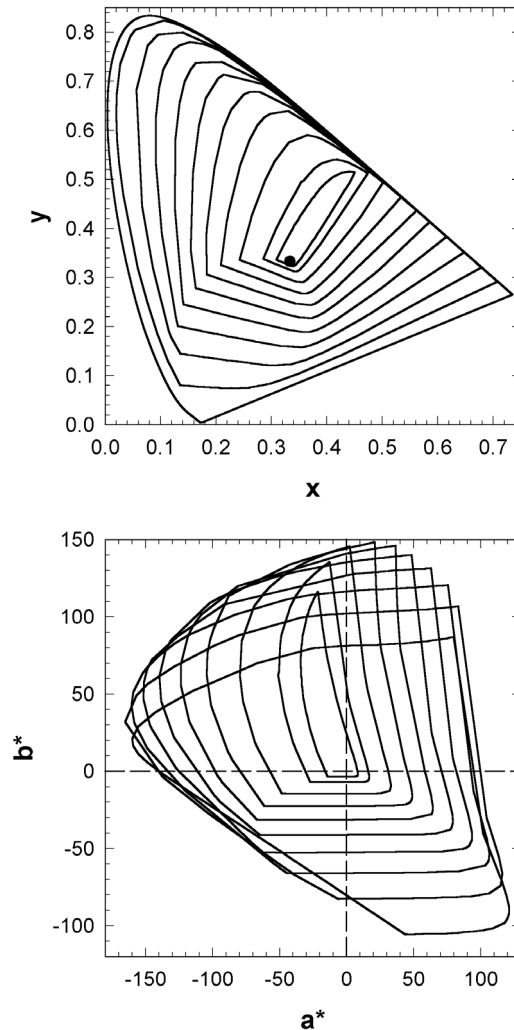
    $end\ for$

$end\ for$

(1)

Figure 2. MacAdam limits under equal-energy illuminant (solid symbol) in the chromatic diagrams CIE-xy (top) and CIE-a*b* (bottom) relative to the luminance factor Y: more external locus (Y = 10), more internal locus (Y = 95).

opto-electronic devices, could just encode virtually these color-stimuli.

Encoding these color-stimuli according to CIE-1931 XYZ standard observer, they are arranged in decreasing pyramidal form as the luminance factor increases (Fig. 2). These loci are often called MacAdam limits or Rösch color solid[1,2] and show the theoretical limits of the chromaticities that (non-fluorescent) colored surfaces or filters can attain for any given total reflectance or transmittance. If we wish to obtain these loci with other illuminant[1,2,4] **L**(A, D65, etc), it is necessary to change in the above equation $\mathbf{T_{XYZ}}$ by $\mathbf{T_{XYZ}} \cdot \text{diag}(\mathbf{L})$ and $\mathbf{E}$ by $\mathbf{L}$ in the scalar product. Therefore, these loci are useful as reference in the industry to improve the gamut of pigments, dyes and inks[5,6].

However, we do not know how other additive capture devices different to the CIE standard observer might encode these optimal colors. Output devices, displays and printers (as subtractive devices), cannot build the optimal colors because its electronic-optical model performs from the internal variables (digital RGB or CMYK data) to a spectral power distribution of light or color-stimulus. On the other hand, input devices (scanners and cameras), like

Using experimental data about the spectral and colorimetric characterization of a digital camera, the purpose of this work is to simulate the RGB capture the optimal color-stimuli and transform these RGB data to XYZ data by means of the raw colorimetric profile associated to the device. Comparing both color gamuts with *Y* fixed, we can inquire whether the digital camera reproduces correctly in general any color-stimulus.

Methodology

The experimental procedure followed is described in Figure 3. The input data are the spectral reflectances of 550 optimal colors under the equal-energy illuminant **E**. The illumination in this scene is 1000 lx, obtained with a

constant spectral radiance **E** equal to 4.36 mW/sr·m². Although these radiometric and photometric data are not necessary to obtain the relative XYZ data by the CIE standard observer (Fig. 2), they are very important to obtain the estimated XYZ data by our digital still camera (DSC).
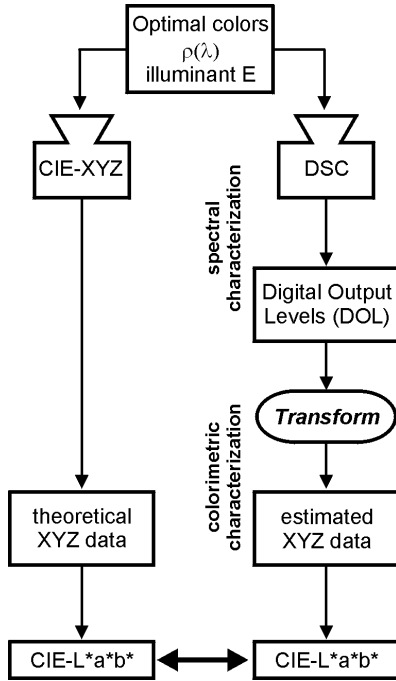

Figure 3. Colorimetric chain for comparing the MacAdam limits between the CIE standard observer and a digital still device.

Color Characterization Model for Digital Cameras

Our digital image capture device consisted of a Sony DXC-930P camera connected to a Matrox MVP-AT 850 frame grabber, inserted into a PC unit. Among the fixed initial conditions, which might alter the color output data, we set the white balance to 5600 K in manual menu-mode (offset value) and configured the gain and the offset of the analog-digital converter in optimal values to alter minimally the camera raw signal. According to the ISO 17321 recommendations[7], the selected initial conditions allowed us to work with the raw response space of the color device.

The color characterization model for this digital camera, valid for any camera, consists of two parts: spectral and colorimetric characterization (Fig. 3).

The purpose of the spectral characterization for a digital image capture device (scanner or camera) is the determination of their spectral sensitivities from spectroradiometric measures in a monochromator set-up. In our case[8], this purpose was achieved using the empirical relationship between the normalized digital output level $NDOL_\lambda$ vs. spectral exposure H_λ for RGB channel, denoted as opto-electronic conversion spectral functions (OECSF).

Considering the spectral exposure $H(\lambda)$ as proportional to the spectral radiance $L_e(\lambda)$ of the target and to the photosite integration time t, and inversely proportional to the square of the f-number N of the zoom-lens, the *OECSFs* curves were fitted mathematically by sigmoid functions (Fig. 4), defined by four parameters $\{a,b,c,d\}$ as follows:

$$H(\lambda) \propto \frac{L_e(\lambda)}{N^2}t$$

$$NDOL_k(\lambda) = \frac{DOL_k(\lambda)}{2^{bits}-1} \quad , \quad k = R,G,B \qquad (2)$$

$$NDOL_k(\lambda) = a_k(\lambda) + \frac{b_k(\lambda)}{1+\exp\left(-\dfrac{H(\lambda)-c_k(\lambda)}{d_k(\lambda)}\right)}$$
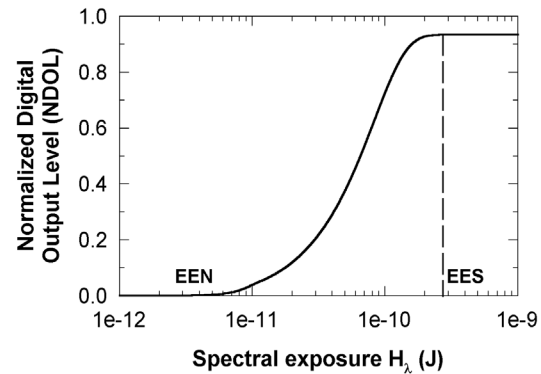

Figure 4. Example of opto-electronic conversion spectral function (OECSF) for any color channel of a digital image capture device. The equivalent exposure noise (EEN) and saturation (EES) points can be seen. The mid-range of response or transition zone between both tails is a straight line using a linear x-axis.

With this radiometric formalism, we will choose the f-number $N = 4$ and the phosite integration time $t = 20$ ms (offset value by camera menu) for our input device. Besides, considering $\Delta\lambda = 10$ nm for our simulation, a new model of capture applied over the optimal colors may be proposed from the univariance principle:

$$DOL_k = \left(2^{bits}-1\right)\sum_{380\,nm}^{780\,nm}NDOL_k(\lambda)\Delta\lambda =$$

$$= \left(2^{bits}-1\right)\sum_{380\,nm}^{780\,nm}\left[a_k(\lambda) + \frac{b_k(\lambda)}{1+\exp\left(-\dfrac{H_{MacAdam}(\lambda)-c_k(\lambda)}{d_k(\lambda)}\right)}\right]\Delta\lambda \quad (3)$$

with $\quad H_{MacAdam}(\lambda) = 2.8e-12 \cdot \rho_{MacAdam}(\lambda)$

The colorimetric characterization consists in transforming the raw RGB digital data into CIE-XYZ tristimulus values (Fig. 3). Thus, at the first stage, a gray balance was applied over the raw RGB digital data to convert them into RGB relative colorimetric values. At a second stage, an algorithm of luminance adaptation[9] vs. f-number of the zoom-lens was inserted in the basic colorimetric profile.

If $NDOL_k$ is the normalized digital output level for each color-channel, the relative RGB values are obtained from the ratio between the areas beneath the color-matching functions associated with the camera. Because this ratio is not 1:1:1 but 0.8642:0.6839:1, the gray balance is applied as follows:

$$R = \frac{NDOL_R}{0.8642} \quad ; \quad G = \frac{NDOL_G}{0.6839} \quad ; \quad B = NDOL_B \quad (4)$$

The basic colorimetric profile[9,10] is a 3x3 matrix $\mathbf{M}$ which should associate the RGB relative colorimetric values or $\mathbf{t_{RGB}}$ with the relative tristimulus values $\mathbf{t_{XYZ}}$ normalized to the equal-energy stimulus or *adapted white* $\mathbf{E} = [1, 1, ..., 1]^t$ (Eq. 2), and not to the *adopted white*, according to the terminology used in ISO 17321[7]. This matrix can be obtained by regression[10] between the color-matching functions $\mathbf{T_{RGB}}$ of our color device and those of the standard observer CIE-1931, $\mathbf{T_{XYZ}}$. In this way, the estimated relative tristimulus values XYZ should be as follows:

$$\hat{\mathbf{t}}_{\mathbf{XYZ}} = \mathbf{M} \cdot \mathbf{t_{RGB}} \quad , \quad \mathbf{T_{XYZ}}^t = \mathbf{M} \cdot \mathbf{T_{RGB}}^t$$

$$\mathbf{M} = \mathbf{T_{XYZ}}^t \cdot \mathbf{T_{RGB}} \cdot \left(\mathbf{T_{RGB}}^t \cdot \mathbf{T_{RGB}} \right)^{-1} = \quad (5)$$

$$= \begin{bmatrix} 1.5798 & 0.4016 & 0.3643 \\ 1.0086 & 1.6157 & 0.0742 \\ -0.0107 & 0.1573 & 2.0189 \end{bmatrix}$$

However, it is necessary to complete this colorimetric profile inserting the inverted camera *OECF* (opto-electronic conversion function[7]) and the luminance L_E (= $1000/\pi$ cd/m^2) of the adapted white as follows:

$$\hat{\mathbf{t}}_{\mathbf{XYZ}} = \frac{1}{L_E} \mathbf{M} \cdot \begin{bmatrix} OECF_R^{-1}(R) \\ OECF_G^{-1}(G) \\ OECF_B^{-1}(B) \end{bmatrix} \quad (6)$$

Simulating the camera responses with the f-number N free to a gray scale test pattern illuminated by equal-energy illuminant, a new luminance adaptation algorithm[9] has been derived to describe the inverted camera *OECFs*. These photometric characterization functions can be approximated as straight lines whose slope m and offset value h are second-order polynomials respect to the f-number N (Table 1). Therefore, from Fig. 3 and following the terminology of ISO 17321 the final colorimetric profile is:

- Original-referred image data (XYZ data relative to 100 of the optimal colors):

$$\mathbf{t_{XYZ}} = \begin{bmatrix} X \\ Y \\ Z \end{bmatrix} \quad (7)$$

- Scene-referred image data (estimated XYZ data relative to 100 of the optimal colors):

$$\hat{\mathbf{t}}_{\mathbf{XYZ}} = \begin{bmatrix} \hat{X} \\ \hat{Y} \\ \hat{Z} \end{bmatrix} = \frac{1}{L_E} \mathbf{M} \left\{ \begin{bmatrix} m_R(N) & 0 & 0 \\ 0 & m_G(N) & 0 \\ 0 & 0 & m_B(N) \end{bmatrix} \begin{bmatrix} R \\ G \\ B \end{bmatrix} + \begin{bmatrix} h_R(N) \\ h_G(N) \\ h_B(N) \end{bmatrix} \right\}$$

$$\text{with} \quad \begin{cases} m_k(N) = m_{0k} + m_{1k}N + m_{2k}N^2 \\ h_k(N) = h_{0k} + h_{1k}N + h_{2k}N^2 \end{cases}$$

$$(8)$$

Table 1. Fitting parameters of the second order polynomial of the slope and the offset value of the inverse camera *OECF* for each color channel as a function of the f-number *N*.

CHANNEL	Slope "m"		
	m_0	m_1	m_2
R	2.9328	-1.1753	16.6933
G	4.2475	-1.7476	16.3244
B	2.1729	-0.7980	16.7543
CHANNEL	Offset value "h"		
	h_0	h_1	h_2
R	-1.8589	0.7488	3.6676
G	-2.5022	1.0540	4.5253
B	-1.3288	0.4843	3.5035

To predict better the scene colorimetry the final step of our color characterization model is to compare the estimated XYZ data with the theoretical XYZ data associated to the optimal colors. This comparison, plotted in Fig. 5, indicates that a color correction is necessary to predict better the scene colorimetry. A linear model of color correction, as in Eq. 9, is the most simple option and it seems that it works well (Fig. 5). This is understandable since due to the mismatch of the $\mathbf{T_{RGB}}$ color matching functions (Luther condition[11-13]) our color device will show systematic color deviations.

$$\mathbf{t_{XYZ}} = \mathbf{A_C} + \mathbf{B_C} \cdot \hat{\mathbf{t}}_{\mathbf{XYZ}}$$

$$\begin{bmatrix} X \\ Y \\ Z \end{bmatrix} = \begin{bmatrix} -21.17 \\ -25.29 \\ -22.96 \end{bmatrix} + \begin{bmatrix} 2.619 & 0 & 0 \\ 0 & 2.765 & 0 \\ 0 & 0 & 2.881 \end{bmatrix} \cdot \begin{bmatrix} \hat{X} \\ \hat{Y} \\ \hat{Z} \end{bmatrix} \quad (9)$$

Although the linear color correction model consists of two factors, one additive (offset vector $\mathbf{A_C}$) and other multiplicative (diagonal matrix $\mathbf{B_C}$), we think that the $\mathbf{B_C}$ can be included in the final colorimetric profile (Eq. 8) to establish the raw colorimetric profile of our input device. We think that this is possible because this parameter, justified by the Grassmann laws, performs like a unnoticed

multiplicative factor necessary to re-adjust the photometric dynamic response of the scene. On the other hand, we think that the offset tristimulus vector $\mathbf{A}_c$, not justifiable by Grassmann laws, is the only parameter describing the systematic color deviations of our color device. That is, it is the error associated (bias) with the difference between theoretical and estimated XYZ data. Since we always have simulated raw RGB data from the camera to avoid the influence of any uncontrolled post-processing, we think that the offset tristimulus vector $\mathbf{A}_c$ should really be the only variable of the color correction model which can be justified by the mismatch of the color matching functions. Therefore, we are going to apply the raw colorimetric profile (without $\mathbf{A}_c$) over the estimated RGB data associated to the optimal colors in order to compare the MacAdam limits between our input device, in raw performance, and the CIE standard observer.

Results and Discussion

From Fig. 6 it can be seen that plotting the theoretical and estimated MacAdam limits in CIE-(a*,b*) chromatic diagram, all the loci associated to our input device are more smaller than the ones of the CIE standard observer. This means that, in raw performance, our input device desaturates the optimal colors, and in general, all the real color-stimuli. From Table 2 it can be seen that our input device also lightens the optimal colors in raw performance because the estimated luminance factors Y (without $\mathbf{A}_c$) are higher than the theoretical ones. This result is consequence of the limited luminance dynamic range (OECSF and OECF) of our color device compared with the standard observer (unlimited). In this simulation, as usual, an attempt has been made to saturate the lighter optimal colors instead of the darker ones.
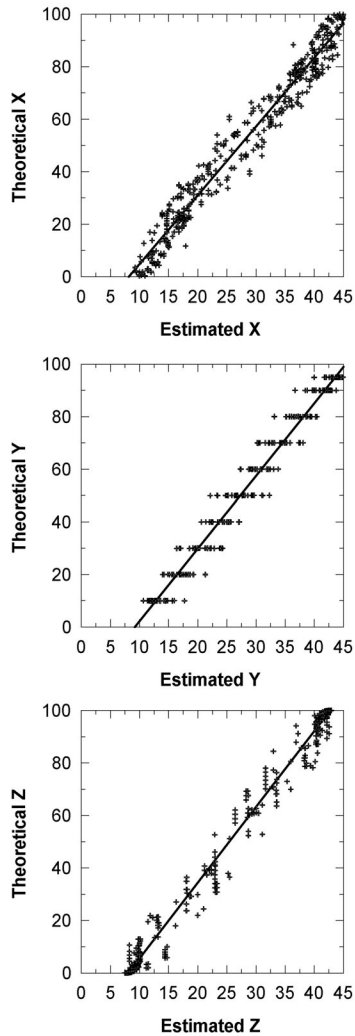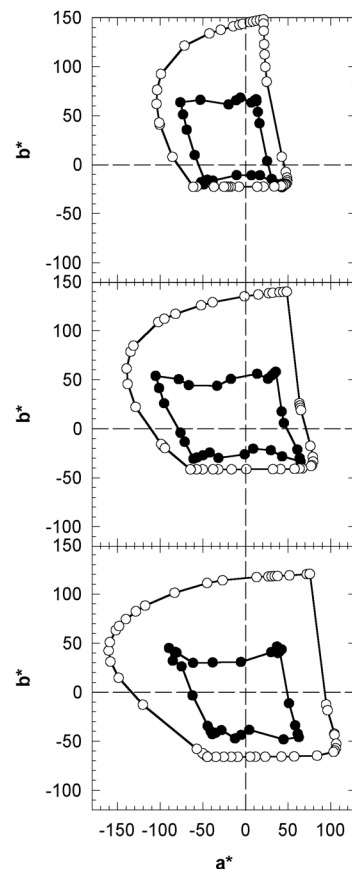

Figure 5. Linear correction (solid line) of the tristimulus values X (top), Y (center) and Z (bottom) of 550 optimal colors (crosshair symbol) using the raw colorimetric profile associated to our digital image capture device.

Figure 6. MacAdam limits with luminance factor Y = 30 (bottom), 50 (center) and 70 (top) in CIE-(a,b*) diagram according to the color encoding of the standard observer (external line with hollow symbols) and our input device (internal line with solid symbols) in raw performance.*

This camera behavior, above all due to the mismatch of the color matching functions of the camera, is very similar to the effect of the Ives-Abney-Yule compromise[14] in relation with the design of the spectral sensitivities of an input device. Since the spectral sensitivities are all positive, although the Luther condition is not fulfilled, this arrangement confines mainly the color errors to excesses of lightness and losses of chroma (Table 2). However, unlike the Ives-Abney-Yule compromise, which uses a non linear correction factor, a tristimulus vector A_C as a linear correction model suffices to reach a good level of exact color reproduction, although improving the lightness more than the chroma.

Table 2. Average absolute color deviations in CIE-L*a*b* space of the raw and corrected (with A_c) reproduction model for 550 optimal colors.

	$|\Delta L^*|$	$|\Delta a^*|$	$|\Delta b^*|$	$|\Delta C^*|$	$|\Delta H^*|$	ΔE	ΔE_{94}
Raw	16.24	25.27	29.21	39.99	13.14	47.41	20.22
Corr.	2.89	14.86	13.38	15.45	13.15	22.46	7.86

Conclusions

Selecting carefully the raw responce space of an input device, a color characterization model has been used to predict its color gamut using the optimal color-stimuli. In this model, the performance of the device has been separated into raw and corrected (with offset tristimulus vector A_C). The results in CIE-L*a*b* color space shows that our input device, in raw performance, lightens and desaturates the optimal colors and, in general, all the real color-stimuli. This result justifies the additional use in digital photography of color correction algorithms, more or less complex, in order to reach the colorimetric status of color reproduction.

Although the term A_C, as only parameter of the color correction model, cannot be justified using the Grassmann laws, we think that this parameter can be justified by the mismatch of the color matching functions. Recalculating the MacAdam limits with the corrected color model for our input device, the estimation of the lightness and chroma improves significantly. Therefore, we think that this experimental procedure can be applied to other digital image capture devices to determine their gamut devices.

Acknowledgements

References

1. D.L. MacAdam, J. Opt. Soc. Amer., 15, 361 (1935).
2. G. Wyszecki & W.S. Stiles, Color Science: Concept and Methods, Quantitative Data, John Wiley & Sons, 1982, New York, 1982, pg. .
3. H.J. Trussell, Color Res. Appl., 16, 31 (1991).
4. R.W.G. Hunt, The Reproduction of Colour, 5th ed., Fountain Press, Kingston-upon-Thames, 1995, pg. 132.
5. M.R. Pointer, Color Res. Appl., 5, 145 (1980).
6. R.S. Berns, Principles of Color Technology, 3rd ed., John Wiley & Sons, New York, 2000, pg. 145.
7. ISO/WD 17321, Graphic Technology and Photography – colour characterization of digital still cameras (DSCs), ISO, Geneva, 2002; http://www.pima.net/standards/iso/tc42/wg20/wg20.htm.
8. F. Martínez-Verdú, J. Pujol & P. Capilla, J. Imaging Sci. and Technol., 46, 15 (2002).
9. F. Martínez-Verdú, et al., Reproduction Model with Luminance Adaptation for Digital Cameras, Proc. CGIV, pg. 529 (2002).
10. G.D. Finlayson, M.S. Drew, J. Electron. Imaging, 6, 484 (1997).
11. R. Luther, Z. Tech. Phys., 8, 540 (1927).
12. H.E. Ives, J. Franklin Inst., 16, 673 (1915).
13. B.K.P. Horn, Comput. Vis. Graph. Image Process., 26, 135 (1984).
14. R.W.G. Hunt, The Reproduction of Colour, 5th ed., Fountain Press, Kingston-upon-Thames, 1995, pg. 128, 453.

Biography

Jaume Pujol received his BS in Physics from the University of Valencia in 1993 and a Ph.D. in Physics from Technical University of Catalonia at Terrassa (Barcelona) in 2001. Since 1998 he teaches Vision Sciences at School of Optics & Optometry in the University of Alicante (Spain). His work is primarily focused on Color Imaging (device calibration and characterization, color management) and Industrial Colorimetry. He is a member of the OSA and the Spanish Optics Society. E-mail: pujol@oo.upc.es.